View metadata, citation and similar papers at core.ac.uk

brought to you by CORE

provided by Institutionelles Repositorium der Leibniz Universität Hannover

IOP Conference Series: Materials Science and Engineering

PAPER • **OPEN ACCESS**

Numerical investigation of a double frequency approach for longitudinal HF welding of cladded pipes

To cite this article: W. Ebel *et al* 2018 *IOP Conf. Ser.: Mater. Sci. Eng.* **424** 012069

View the article online for updates and enhancements.

IOP ebooks™

Bringing you innovative digital publishing with leading voices to create your essential collection of books in STEM research.

Start exploring the collection - download the first chapter of every title for free.

This content was downloaded from IP address 194.95.159.70 on 30/08/2019 at 11:49

Numerical investigation of a double frequency approach for longitudinal HF welding of cladded pipes

W.Ebel[1], M.Kroll[2], E.Baake[1], A. Nikanorov[1]

[1] Institute of Electrotechnology, Leibniz Universität Hannover,
Wilhelm-Busch-Str. 4, D-30167 Hannover, Germany

[2] Institute for Machine Tools and Production Processes, Technische Universität Chemnitz
Reichenhainer Str. 70, D-09126 Chemnitz, Germany

Corresponding author: baake@etp.uni-hannover.de

Abstract
This article contains findings of simulation research on longitudinal induction welding of cladded pipes with use of simultaneous double frequency. Solutions are proposed to reach the required temperature distribution at the welding edge for the cladding composite of S355 and Alloy 625 with single and simultaneous double frequency. An advanced consideration of magnetic and other material properties was performed to simulate the dominating physical effects of high frequency (HF) welding. The background of use and advantages of simultaneous double frequency are presented. In the context of the research, a correlation for welding speed, frequency and temperature distribution with industrial relevance was found for the cladded pipe welding.

Key words: HFI-welding, longitudinal welding, pipes, cladded pipes, induction welding

Introduction

Today, cladded pipes are used in niche applications in natural gas transportation systems, power plants and the chemical industry. The combination of two different metals within one pipe offers high corrosion and abrasion resistance in an economical way. Until today the cladded pipes are manufactured by discontinuous arc welding, weld cladding or mechanical bracing with comparatively low production rates. Bended cladded sheet material, which is metallurgically bonded by explosive cladding, cold roll or hot roll bonding, serves as the feedstock for the welding process. Induction heating is a state of the art process in longitudinal seam welding of single material pipes. It is widely used in the almost all industries. Despite its very high productivity (feed speed of up to 200 m/min [2]) and energy efficiency, inductive longitudinal seam welding is not applied in the manufacturing of cladded pipes. With less than 5 m/min [3], [4] arc welding as the conventional joining process is far less productive.
In this paper, a 2D model of pipe welding is used to examine the dominating process parameters for a common material combination of the fine-grained ferritic carbon steel S355 and the nickel base Alloy 625. S355 exhibits a good weldability and is applied as an outer carrier material. The inner layer of Alloy 625 is characterised by a great resistivity against all kinds of corrosion.

Solution Approach

In this work, a 2D dynamic model is created to determine the influence of the main pipe welding parameters, such as feed rate, Vee angle, distance of inductor to the welding point, geometry of cross sections and the electrical parameters. The dynamic model is able to represent the 3D induction welding as shown in [5]. This can be done, as due to proximity effect, where the inductor have only a localized effect on current distribution, but a weak effect on the welding edge current.

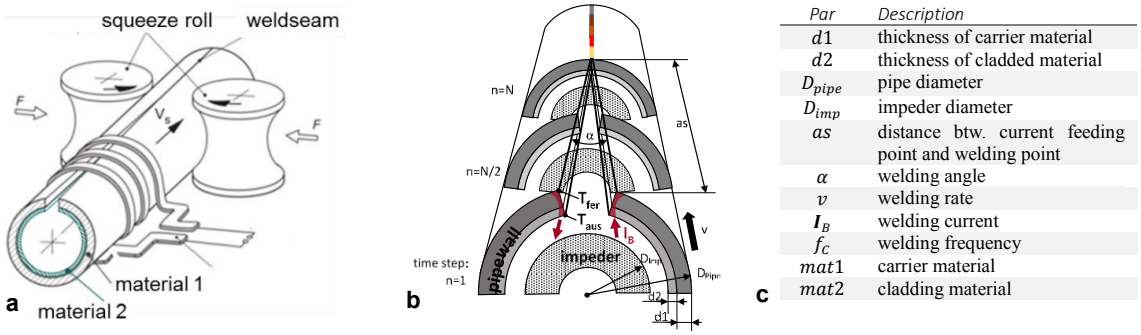

c

Par	Description
$d1$	thickness of carrier material
$d2$	thickness of cladded material
D_{pipe}	pipe diameter
D_{imp}	impeder diameter
as	distance btw. current feeding point and welding point
α	welding angle
v	welding rate
I_B	welding current
f_C	welding frequency
$mat1$	carrier material
$mat2$	cladding material

Fig. 1. Overview of inductive pipe welding process (a), 2D model steps along the pipe edge move (b) model parameters considered by the simulation (c)

Content from this work may be used under the terms of the Creative Commons Attribution 3.0 licence. Any further distribution of this work must maintain attribution to the author(s) and the title of the work, journal citation and DOI.
Published under licence by IOP Publishing Ltd

The basic geometries of the inductive welding is shown in Fig. 3 a, the model geometry and considered parameters for the numerical research in Fig. 1 b, c. The solution was calculated by a weak electromagnetic – thermal coupling algorithm in the commercial FEM software ANSYS® Mechanical as shown in [6]. After each time step the results were transferred between the electromagnetic and thermal solutions. The electromagnetic solution was calculated in several iterations to adapt the magnetic permeability according to magnetic field strength.

Material Properties and Influence

Electro- and thermo-physical properties of the cladded pipe materials are pivotal to reproduce the physical effects in the simulation. Due to the non-linearity of the material parameters for the alloys used, the process behaviour is highly sensitive to the change of any input properties. To obtain precise results, physical properties of used material need to be considered and determined from ambient temperature to the melting (or liquefaction) point. In this context, the specific electrical resistance and the thermal conductivity are considered as shown in Fig. 2 a, b.

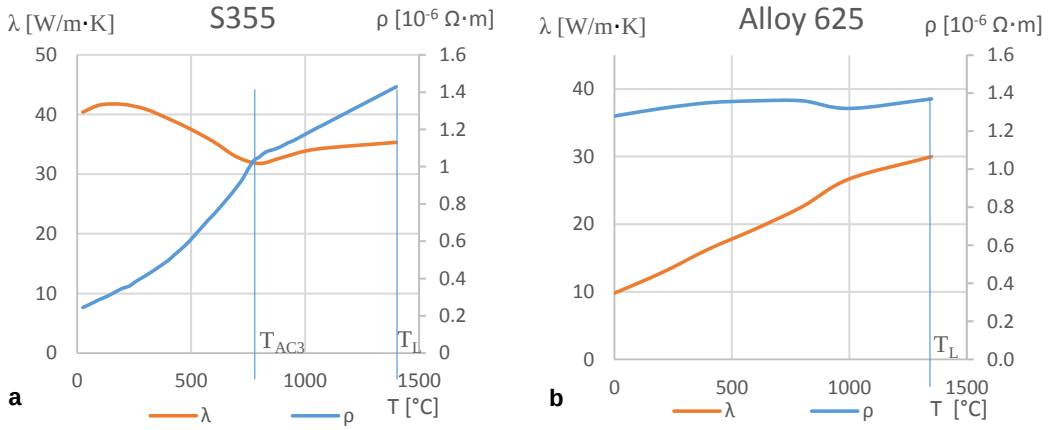

Fig. 2. Specific electrical resistance ρ and thermal conductivity λ of S355 [9], [13] (a) and Alloy 625 [10] (extrapolated to the melting points) (b)

The liquefaction temperatures of the alloys used are given as $T_L(\mathrm{S355}) = 1471°\mathrm{C}$ [7] and $T_L(\mathrm{Alloy\ 625}) = 1340°\mathrm{C}$ [8]. The function for the temperature dependent specific heat capacity for each alloy [9], [10] is complemented by the enthalpy of the fusion distribution function $h(T)$, which integral equalizes the enthalpy of fusion value L_f. The heat of fusion is calculated by the pure element enthalpy of fusion and the mass proportion of each element in the alloy. For the S355, the heat of fusion is determined as $L_{f,S355} = 266\ kJ/kg$ which is close to reference value $L_{f,S355,lit} = 268\ kJ/kg$ [11]. For the nickel-based Alloy 625, the enthalpy of fusion is calculated as $L_{f,A.625} = 338.4\ kJ/kg$.

In the context of material precision, a particular look on the relative magnetic permeability of the backing steel S355 and the ferrite material of the impeder is made. Except the consideration of temperature depending change up to the Curie temperature, magnetic field dependence must also be taken into account. Equation (**1**) is an approximation function for the real part of magnetic permeability μ_r', introduced by Fisher [12, pp. 286–299] and transferred from the magnetic flux B(H) to the relative magnetic permeability $\mu_r(H)$ relation. By choosing $a_F = 390$ and $b_F = 0.697$ [13, p. 67] as coefficients for the soft magnetic material S355 [14], the magnetic field dependency of material S355 is taken into account. For the impeder an adapted magnetic saturation function, with a starting pitch is used as shown in Fig. 3 b.

$$\mu_r'(H) = \frac{1}{\mu_0(a_F + b_F * |H|)} \tag{1}$$

For the temperature-field dependence of the magnetic permeability, equation (2) is used, with a function φ(T) representing the temperature dependence of the permeability. This function is taken from [15, p. 76] and redrawn in (Fig. 3 c).

$$\mu_r(H, T) = \varphi(T) * (\mu_r(H) - 1) + 1 \tag{2}$$

The saturation effect is correlated with the welding current and can be indirectly used for the process control by two input parameters. The change of current frequency influences the electromagnetic skin depth and therefore the required welding current. The second influence on the saturation is the welding rate, which is also positively correlated to the required current. Due to the complexity of the process, both input parameters have side effects. For example, a lower feed rate increases the effect of the divergent heat conductivity of materials by extending the process time.

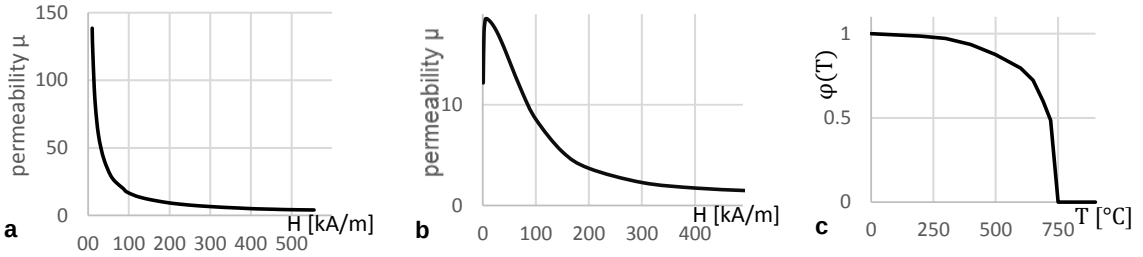

Fig. 3. Magnetic field dependent permeability of S355 at 20°C (a), permeability of the ferrite impeder (b) and temperature dependent function of permeability φ(T) referring to [15, p. 76] (c)

The 2D dynamic model has some limitations in the representation of the process: For example the longitudinal heat transfer and effect of adverse current circuit on the pipe inside cannot be displayed. Despite this the model represents the main physical effects of welding in the cross section and can be used for the task of finding matching process parameters.

Single Frequency Welding

The correct simulation of the welding of cladded pipes strongly relates to the material properties and their proportion to each other. The temperatures T_{fer} for the S355 and T_{aus} (Fig. 1 b) for the Alloy 625 at both edges of the joint serve as the target variable (Fig. 1 b). The aim is to reach the liquefaction temperature of both alloys when the joining surfaces get in contact. Welding with single frequency (SF) is possible by adapting the frequency and the feed rate to the geometrical parameters. Therefore, a feed rate – frequency curve can be found for each material combination and geometrical setup. For a given setup (Fig. 4 a) a corresponding correlation of feed rate – welding velocity is presented in Fig. 4 b.

a

Parameter	*Value*
$d1$	$2\ mm$
$d2$	$1\ mm$
D_{pipe}	$60\ mm$
D_{imp}	$42\ mm$
as	$90\ mm$
α	$2°$
$mat1$	$S355$
$mat2$	$Alloy\ 625$

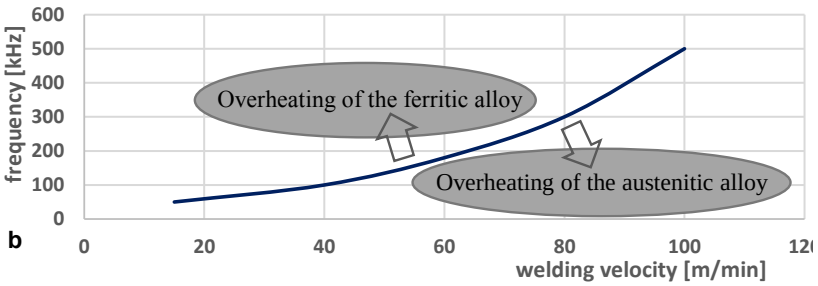

Fig. 4. Geometrical and material parameter set for single frequency simulation (a), frequency – welding velocity curve for convenient welding temperature at the join edge

As shown in Fig. 4 b, the frequency should match the chosen welding speed to melt both alloys at the desired position. Industrial welding generators usually do not offer the high enough flexibility to adapt the frequency in a wide range to the demanded feed rate in practical use. Therefore, the use of double frequency for the longitudinal welding of cladded pipe was investigated.

Simultaneous Double Frequency Welding

Welding with two simultaneous frequencies permits a higher flexibility for the operative adaptation of the welding process to industrial scale variations in pipe geometry and material. For a fixed geometrical and material setup, the usable range of feed speeds depends on the spread of the upper and lower frequency of the energy source.

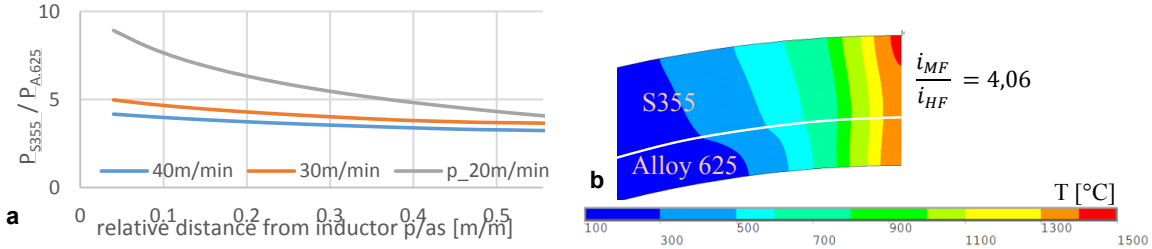

Fig. 5. Total power proportion between the layers for different welding velocities (a), resulting temperature distribution for the welding velocity of $v = 40\ m/min$

To lower the welding speed, it is necessary to increase the relative absorbed power in the ferritic steel layer in proportion to the austenitic alloy. This is necessary as the ferritic S355 offers a higher heat conductivity (Fig. 5 a). The examined frequencies for the research are $f_{HF} = 220\ kHz$ for upper and $f_{MF} = 10\ kHz$ for the lower frequency. From Fig. 4 it can be taken, that with the chosen frequencies the minimum and maximum welding velocities are $v_{min} = 10\ m/min$ and $v_{max} = 68\ m/min$. For the welding velocity of $v = 40\ m/min$, the desired temperature distribution can be reached by setting a MF to HF current ratio of $i_{MF}/i_{HF} = 4{,}06$ (Fig. 5). Further suitable material combinations, such as S235 for the carrier material and X5CrNi18 or X2CrNiMo17 as cladding materials, can be found for the presented longitudinal seam welding approach.

Conclusion

By the use of FEM analysis, the theoretical capability of an inductive longitudinal seam welding process for cladded pipes can be demonstrated. Despite some simplification, the main dominating effects of the longitudinal seam welding were considered by the developed model. Industrial scale process windows for both, single frequency and simultaneous double frequency are presented in this work. The verification was performed on a cladding material combination of S355 and Alloy 625 with strongly divergent material properties, where several effects were used to reach the melting temperatures in the joint edges. The developed approach was also applied to other material combinations, which are not presented in this paper. Potentially, a wide range of metal combinations comprising ferritic alloys as carrier and austenitic alloys as cladding material can be welded by the presented approach. Therefore, a precise material properties determination needs to be existent. Future investigations will highlight the influence of inductor and the full 3D model. Also, thicker-walled cladded pipes are about to be examined for the inductive HF welding.

Acknowledgment

The IGF-project 19041 BG / FOSTA No. P 1183 of the Research Association for Steel Application (FOSTA) was supported by German Federation of Industrial Research Associations (AiF) in the frame of the Industrial Collective Research program (IGF) from Federal Ministry for Economic Affairs and Energy.

References

1. B. Nacke and E. Baake, *Induktives Erwärmen*. Essen: Vulkan Verlag GmbH, 2014.
2. B. Grande and O. Waerstad, “Consistent quality in high-frequency tube and pipe welding,” 2011.
3. X. Meng, G. Qin, Y. Zhang, B. Fu, and Z. Zou, “High speed TIG-MAG hybrid arc welding of mild steel plate,” *J Mater Process Technol*, vol. 214, no. 11, pp. 2417–2424, 2014.
4. J. Sabbaghzadeh, M. Azizi, and M. J. Torkamany, “Numerical and experimental investigation of seam welding with a pulsed laser,” *Opt Laser Technol*, vol. 40, no. 2, pp. 289–296, 2008.
5. A. Nikanorov, E. Baake, H. Brauer, and C. Weil, “Approaches for Numerical Simulation of High Frequency Tube Welding Process,” in *Modelling for Electromagnetic Processing*, 2014, no. 1, pp. 445–450.
6. W. Ebel, M. Kroll, A. Nikanorov, and E. Baake, “Nummerische Simulation des HF-Längsnahtschweißens,” *Prozesswärme*, vol. 2, 2018.
7. E. Le Guen, M. Carin, R. Fabbro, F. Coste, and P. Le Masson, “3D heat transfer model of hybrid laser Nd:Yag-MAG welding of S355 steel and experimental validation,” *Int J Heat Mass Transf*, vol. 54, no. 7–8, pp. 1313–1322, 2011.
8. Corrosion Materials, “Alloy 625,” 2008. [Online]. Available: www.corrosionmaterials.com.
9. U. Peil and M. Wichers, “Schweißen unter Betriebsbeanspruchung – Werkstoffkennwerte zur Temperaturfeldberechnung für einen S 355 J2 G3,” *Stahlbau*, vol. 74, no. 11. pp. 249–257, 2005.
10. M. Woite GmbH, “2.4856,” 2017. [Online]. Available: http://woite-edelstahl.info/24856de.html.
11. J. Winczek and E. Gawrońska, “The modeling of heat affected zone (HAZ) in submerged arc welding (SAW) surfacing steel element,” *Metalurgija*, 2016.
12. J. Fischer and H. Moser, “Die nachbildung von Magnetisierungskurven durch einfache algebraische oder transzendente Funktionen,” *Arch für Elektrotechnik*, vol. 42, no. 5, pp. 286–299, 1956.
13. C. Nörenberg, “Bestimmung elektromagnetischer Materialeigenschaften für Rohrstähle mit Hilfe experimenteller Untersuchungen und numerischer Simulation.,” Leibniz Universität Hannover, 2017.
14. K. Lim and M. Hammond, “Universal Loss Chart for the Calculation of Eddy Current Losses in Thick Steel Plates,” *Proc Inst Electr Eng*, vol. 117 (4), pp. 857–864, 1970.
15. B. Nacke, “Ein Verfahren zur numerischen Simulation induktiver Erwärmungsprozesse und dessen technische Anwendung.. Universität Hannover,” Leibniz Universität Hannover, 1987.